Agarose Fluid Gels Formed by Shear Processing During Gelation for Suspended 3D Bioprinting

Senior, Jessica J.; Moakes, Richard; Cooke, Megan E; Moxon, Sam; Smith, Alan M; Grover, Liam

DOI:
10.3791/64458

jove

Agarose Fluid Gels Formed by Shear Processing During Gelation for Suspended 3D Bioprinting

Jessica J. Senior[*,1], **Richard J. A. Moakes**[*,2], **Megan E. Cooke**[3], **Samuel R. Moxon**[4], **Alan M. Smith**[1], **Liam M. Grover**[2]

[1] Department of Pharmacy, University of Huddersfield [2] School of Chemical Engineering, University of Birmingham [3] Chemical and Biological Engineering, University of Colorado Boulder [4] School of Biological Sciences, University of Manchester

[*] These authors contributed equally

Corresponding Authors

Alan M. Smith
a.m.smith@hud.ac.uk

Liam M. Grover
l.m.grover@bham.ac.uk

Citation

Senior, J.J., Moakes, R.J.A., Cooke, M.E., Moxon, S.R., Smith, A.M., Grover, L.M. Agarose Fluid Gels Formed by Shear Processing During Gelation for Suspended 3D Bioprinting. *J. Vis. Exp.* (195), e64458, doi:10.3791/64458 (2023).

Date Published

May 26, 2023

DOI

10.3791/64458

URL

jove.com/video/64458

Abstract

The use of granular matrices to support parts during the bioprinting process was first reported by Bhattacharjee et al. in 2015, and since then, several approaches have been developed for the preparation and use of supporting gel beds in 3D bioprinting. This paper describes a process to manufacture microgel suspensions using agarose (known as fluid gels), wherein particle formation is governed by the application of shear during gelation. Such processing produces carefully defined microstructures, with subsequent material properties that impart distinct advantages as embedding print media, both chemically and mechanically. These include behaving as viscoelastic solid-like materials at zero shear, limiting long-range diffusion, and demonstrating the characteristic shear-thinning behavior of flocculated systems.

On the removal of shear stress, however, fluid gels have the capacity to rapidly recover their elastic properties. This lack of hysteresis is directly linked to the defined microstructures previously alluded to; because of the processing, reactive, non-gelled polymer chains at the particle interface facilitate interparticle interactions-similar to a Velcro effect. This rapid recovery of elastic properties enables bioprinting high-resolution parts from low-viscosity biomaterials, as rapid reformation of the support bed traps the bioink *in situ*, maintaining its shape. Furthermore, an advantage of agarose fluid gels is the asymmetric gelling/melting transitions (gelation temperature of ~30 °C and melting temperature of ~90 °C). This thermal hysteresis of agarose makes it possible to print and culture the bioprinted part *in situ* without the supporting fluid gel melting. This protocol shows how to manufacture agarose fluid gels and demonstrates their use to support the production of a range of complex hydrogel parts within suspended-layer additive manufacture (SLAM).

Introduction

Hydrogels are perfect materials to use as supports for cell growth[1]. Depending on the material that is used, they gel *via* gentle mechanisms that do not compromise cell viability[2,3]. The high water content (typically >90%) means that nutrients and oxygen can readily diffuse into the material and waste products of cell metabolism diffuse out[4]. As such, cell viability has been shown to be preserved for periods in excess of 1 year[5], and there are now examples of hydrogels being used to store or "pause" cells for future therapeutic use[6]. They have been widely used in tissue engineering for the production of tissue-like structures, but their use tends to be limited by the difficulty in controlling both the structure and composition of the material. Historically, hydrogel strength is comparatively low (in relation to many hard tissues), due to the high water content and low volumes occupied by the polymer matrix forming the structure. Furthermore, many routes to gelation (thermal, ionotropic, fibrillogenesis) offer reasonably slow kinetics, meaning their mechanical properties tend to develop steadily with time. With the exception of interpenetrating networks, low mechanical rigidity and slow curing times often result in bioinks that are unable to free-stand on deposition, tending to "slump" and lose definition when initially extruded.

In an attempt to overcome this key issue, embedded printing techniques have been developed that provide support during printing, while the mechanical properties of the construct are developing[7,8]. Once the microstructure of the gel has fully developed and the mechanical properties reach an optimum, the support matrix can be removed, typically through gentle washing or melting of the support phase. Initial work on this approach utilized a viscous pluronic dispersion in which the secondary phase was distributed[9]. More recently, Bhattacharjee et al. used gels in the form of granulated carbopol to demonstrate that arrays of cells could be suspended in the supporting gel[10]. Subsequently, Hinton et al. reported on the extrusion of gel-based materials containing cells into a support bed that consisted of a microgel suspension formed from granular gelatin[11]. After extrusion of the cell-containing hydrogel and its subsequent curing, the gelatin was removed by gentle heating of the support bath, enabling melting of the gelatin. Unfortunately, this process still presents several limitations. For example, the chemical structure of gelatin in comparison to collagen (consequently to it being a hydrolyzed form of collagen) is such that many chemical moieties across its backbone can interact with biological entities; thus, a residual support matrix could interfere with downstream biological processes. Moreover, animal-derived products pose restrictive use when looking toward the translatability of a technology. This creates challenges if the manufactured part is intended to be used clinically, or even if it is to be used to answer fundamental biological questions, where this surface contamination can cause a significant issue.

We have subsequently created a refined process that allows for the suspended manufacture of hydrogels, within a supportive matrix, that has no charge under physiological conditions and is formed from non-animal materials. Although the process can be used with a range of biopolymeric supports, agarose provides a material that is inert to biological interactions as it is sugar-based and neutrally charged at physiological pH[12,13]. Rather than fragmenting an already existing gel, the support material is formed through the application of shear during gelation[14,15,16]. This produces a matrix of particles that exhibit dendron-like features at their surface and are dispersed in a secondary matrix

of ungelled polymer[17,18]. The result is a material with interesting material properties[19,20,21,22] that can shear-thin in a similar way to previously reported granular gels, but tends to recover viscosity more rapidly when shear is removed[23]. Once the cell-bearing material extruded into the supporting matrix has fully matured, the support matrix can be removed through gentle agitation before being placed in culture. It has been shown that it is possible to use this process to produce materials with complex structures and recapitulate the biological structures of both skin and the osteochondral region[23,24,25]. This methods paper describes in detail how to manufacture the supporting material and highlights appropriate bioinks used within a variety of complex structures.

Protocol

NOTE: See the **Table of Materials** for details related to all materials, reagents, equipment, and software used in this protocol.

1. Preparation of the fluid gel suspension bed

1. Prepare 1,000 mL of dispersed agarose (0.5% w/v) by adding 5 g of agarose powder to 1,000 mL of ultrapure water (Type 1, >18 $m\Omega \cdot cm^{-1}$) in a 2,000 mL glass bottle.
2. Add a 70 mm magnetic stirrer bar to the aqueous mixture and secure the bottle cap by first fully tightening and then loosening by a quarter turn.
3. Dissolve and sterilize the mixture by placing the glass bottle into the basket of the autoclave, closing the lid, and running a cycle for 15 min at 121 °C and 1 Bar.
   NOTE: This protocol is always used for autoclaving solutions in further steps.
4. Remove the bottle from the autoclave once the autoclave has cooled to 80 °C and place it on a magnetic stirrer (unheated), with the stirring set to 800 rpm.
   CAUTION: The bottle and the liquid remain hot.
5. Cool the sol under ambient conditions, while maintaining constant stirring, until the temperature is lower than its T_{gel} (gelling point), 32 °C.
6. Remove the bottle from the stirrer and store it at 4 °C.
   NOTE: The fluid gel can be stored until needed.

2. Preparation of bioinks

1. Prepare a gellan-based bioink using a 1% (w/w) sol of low acyl gellan gum in ultrapure water (Type 1, >18 $m\Omega \cdot cm^{-1}$).
   1. Weigh out 0.5 g of gellan powder into a weighing boat.
   2. Add 49.5 g of ultrapure water into a 100 mL glass bottle, along with a magnetic stirrer.
   3. Fold the weighing boat containing gellan power in half and add the powder to the water slowly, while constantly stirring.
   4. Dissolve and sterilize the sol using an autoclave and allow it to cool to 20 °C.
   5. Store the bioink at 4 °C until further use.
2. Prepare a pectin-collagen blended bioink in ultrapure water (Type 1, >18 $m\Omega \cdot cm^{-1}$).
   1. Prepare stock 5% (w/v) low-methoxy pectin solutions by weighing out 2.5 g of pectin powder into a weighing boat.
   2. Add 50 mL of ultrapure water into a 100 mL glass bottle, along with a magnetic stirrer.

3. Fold the weighing boat containing pectin power in half and add the powder to the water slowly, while constantly stirring.
4. Autoclave the aqueous mixture and cool to 20 °C.
5. Prepare 1:1 and 2:1 pectin-collagen blends by either adding 3 mL of the pectin solution to 3 mL of collagen solution or by adding 4 mL of the pectin solution to 2 mL of collagen solution, respectively. Gently mix the blends using a pipette, by withdrawing and dispensing the mixture 10x.
   NOTE: This procedure is best undertaken using cold materials on ice to prevent premature gelation of the collagen. Precooling of pectin and collagen can be achieved by storing at 4 °C prior to mixing.
6. Store at 4 °C until further use.

3. Prepare an alginate-collagen blended bioink in ultrapure water (Type 1, >18 $m\Omega \cdot cm^{-1}$).
   1. Weigh out 2 g of alginate powder into a weighing boat.
   2. Add 50 mL of ultrapure water into a 100 mL glass bottle, along with a magnetic stirrer.
   3. Fold the weighing boat containing alginate power in half and add the powder to the water slowly, while constantly stirring.
   4. Heat the dispersion to 60 °C, under constant stirring, until the alginate is fully dissolved (clear, slightly brown liquid), and then cool to 20 °C.
   5. Dilute the alginate solution with cell culture medium such as Dulbecco's modified eagle medium (DMEM) by adding 25 mL of the alginate solution to 25 mL of DMEM.
   6. Prepare alginate-collagen blends (1:1) by adding 3 mL of the alginate/DMEM solution to 3 mL of collagen solution. Gently mix the blends using a pipette by withdrawing and dispensing the mixture 10x and store at 4 °C.
      NOTE: This procedure is best undertaken using cold materials on ice to prevent premature gelation of the collagen. Precooling of pectin and collagen can be achieved by storing at 4 °C prior to mixing.

3. Rheological characterization of bioinks

1. Turn on the rheometer, insert 40 mm serrated geometries, and allow to stand for 30 min.
2. Zero the gap height of the rheometer using the **zero-gap height function**.
3. Add ~2 mL of sample on the bottom plate and lower the top geometry to create a gap height of 1 mm.
4. Trim the sample by removing excess material expelled from between the plates. To do this, use a flat, non-abrasive edge to pull excess fluid away from the gap and soak up with tissue paper.
   NOTE: Steps 3.2-3.4 are repeated to change the sample before each of the following steps.
5. Undertake **viscometry profiles** to determine the injectability of the bioink.
   1. Select **viscometry test** from the **user** options.
   2. Input the parameters for a shear rate-controlled ramp test: **0.1 to 500 s^{-1}**, with a **1 min ramp time**.
   3. Repeat the viscometry ramp test on new samples under stress control, using the upper and lower stresses determined from the shear rate-controlled ramp test in step 3.5.2.

6. Undertake **small deformation tests** to determine the gelling characteristics of the bioink.
    1. Select **oscillatory testing** from the **user** options.
    2. Input parameters into a single frequency test under constant strain: **frequency 1 Hz, strain 0.5% over 1 h**, while the ink gels.
7. Undertake *in situ* amplitude and frequency measurements on gelled samples.
    1. Select **oscillatory test** from the **user** options.
    2. Select amplitude sweep and input the parameters for an amplitude sweep test that is strain-controlled: **0.01 to 500%**, at a **constant 1 Hz** frequency.
    3. Load a new sample and select **oscillatory test** from the **user** options. Then, select **frequency test**, and input frequency parameters between **0.01** and **10 Hz** and a strain that is within the linear viscoelastic region (LVR) of the spectra determined from the amplitude sweep data obtained in step 3.7.2 (typically a value between 50% and 80% of the LVR).

4. Designing and printing 3D structures using a 3D bioprinter

1. Launch **CAD Software** to start the generation of a CAD model.
    1. Select **Tools | Materials** in the CAD software to define the printing parameters for the chosen bioink.
    2. Input printing parameters relevant to the printer being used; for example, for the 3D Discovery, input the **estimated filament diameter** (~200-500 µm for most bioinks) in the **thickness** tab to determine the Z thickness of each layer.

        NOTE: Delamination of the final construct is indicative of a need to increase the thickness value, while loss of resolution highlights the need to reduce thickness.
    3. Design the desired structure layer by layer using the **Layer** tabs in the software. **Group** the layers using the Group tab and assign each layer to a level on the Z plane using the **Level** tab.
        1. For example, to generate a lattice structure (using an alginate-collagen blended bioink prepared in step 2.3), create one layer with the filaments along the x axis and a second layer with the filaments along the y axis. Assign both to a separate **Level**.
    4. Under the **Group** tab, determine the build height by selecting the number of repeated units in the structure.
    5. Click the **Generate** tool to create a G-code for the design and view a 3D render of the structure.
2. Close **BioCAD** and launch the **3D Discovery human-machine interface** (HMI) software to initiate the printing process.
    1. Assemble the printhead according to the manufacturer's instructions. Mount the microvalve to the printhead and screw in the chosen extrusion nozzle.
    2. Click the **Needle Length Measurement** function to calibrate the printhead.
    3. Load a culture vessel (e.g., a 6-well plate) onto the printing platform.
    4. Aliquot the bioink into the printing cartridge and screw into the printhead above the micro-valve.

5. Connect the assembled printhead to the pneumatic pressure system and select **printhead on the HMI** to engage.
6. Click **check pressure** to allow tuning of the extrusion pressure.
7. Once an appropriate pressure has been selected (**~30-120 kPa** depending upon the desired resolution), open the **G-code** generated previously and click **Run** to initiate the printing process.

5. Preparation of skin analogues

1. Culture human dermal fibroblasts (HDFs) and adipose-derived stem cells (ADSCs) in DMEM supplemented with fetal bovine serum (FBS) (10%), HEPES buffer (2.5%), and penicillin/streptomycin (1%) in T75 flasks until 90% confluency is reached. Culture human epidermal keratinocytes (HEKs) in keratinocyte growth media (KGM) until 70%-80% confluency is reached. Keep all cells under conditions of 37 °C, 5% CO_2, and 95% air in an incubator during culture.
2. For the preparation of HDFs and ADSCs for dermal and adipose bioinks, wash the cells by gently pipetting 3 mL of phosphate-buffered saline (PBS) into flasks, tilt the flask to swirl the PBS over the cells, and aspirate, taking care not to disturb the attached cells.
    1. To lift the cells, pipette 3 mL of 1x cell dissociation enzyme into the flask to cover the cells and place the flask in an incubator for 3 min, firmly tapping the flask against the palm of the hand to dislodge the cells. Neutralize the action of the enzyme using 6 mL of complete DMEM.
    NOTE: Incubate for a further 2 min if the cells remain attached after tapping.
    2. For the preparation of the dermal and adipose bioinks, pipette the cell suspensions into separate 15 mL tubes and take 10 µL from each for cell counting using a hemocytometer. Centrifuge the remaining cell suspensions at 300 × *g* for 5 min to pellet the cells.
    3. Aspirate the supernatant, being careful not to disturb the pellet, add the appropriate polymer solution (prepared in step 2.2), and mix using gentle stimulation by pipetting at the following densities:
        1. For the adipose layer, pipette 5×10^5 ADSCs mL^{-1} per 1:1 collagen to pectin blend.
        2. For the papillary layer, pipette 3×10^6 HDFs mL^{-1} per 2:1 collagen to pectin blend.
        3. For the reticular layer, pipette 1.5×10^6 HDFs mL^{-1} per 2:1 collagen to pectin blend.
3. To print, load each bioink into a separate cartridge and print the construct in the supporting fluid gel in a glass Petri dish according to the instructions in section 4.
    1. Once printing is complete, inject 2 mL of 200 mM $CaCl_2 \cdot 2H_2O$ around the construct and 3 mL of adipogenic media (complete DMEM supplemented with 500 µM isobutyl-methylxanthine [IBMX], 50 µM indomethacin, and 1 µM dexamethasone) into the fluid gel using a syringe and needle. Place in an incubator overnight.
    2. The following day, remove the construct from the support bath using a spatula, gently wash in PBS, and culture for 14 days in adipogenic medium in a 6-well plate.

3. After 14 days, remove enough medium to create an air-liquid interface at the surface of the construct and seed 2 × 10^6 keratinocytes atop the construct to create an epidermal layer.
4. Culture further for 1 week prior to analysis.

6. Preparation of carotid artery model

1. Load the gellan gum bioink solution (as prepared in step 2.1) into a printer cartridge.
2. Print the carotid artery model within a Petri dish containing the fluid gel support material according to the printing instructions in section 4.
3. Once printing is complete, inject 2 mL of 200 mM $CaCl_2{\cdot}2H_2O$ around the construct using a syringe and needle.
4. After a minimum of 3 h, remove the construct from the support bath using a spatula and gently wash in PBS.

Representative Results

Alginate and type I collagen bioink

Print resolution (recorded as a function of filament diameter) was observed to be directly tunable *via* changes in extrusion pressure (**Figure 1A-C**). Extrusion pressure and print resolution were directly related to the smallest filament diameters generated *via* printing at an extrusion pressure of 30 kPa. Interestingly, at an extrusion pressure of 30 kPa, filaments that matched the inner diameter of the extrusion nozzle could be generated (mean filament diameter: 323 µm ± 50 µm; nozzle diameter: 300 µm), suggesting that a "maximum resolution" could be achieved. Moreover, the printing parameters for this resolution could be successfully applied to the generation of an alginate/collagen vascular tube that can be extracted and perfused (**Figure 1D**).

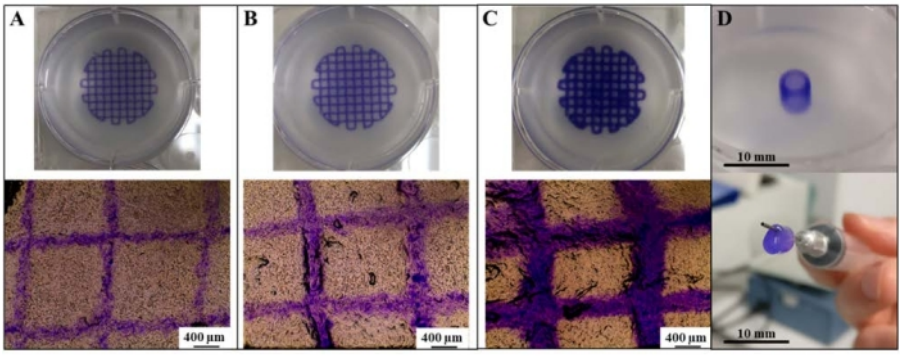

Figure 1: Generation of high-resolution prints using SLAM. Tailoring print resolution of alginate/collagen lattices as a function of filament diameter *via* extrusion at (**A**) 30 kPa, (**B**) 60 kPa, and (**C**) 120 kPa. (**D**) Generation of an alginate/collagen vascular tube. Scale bars = 400 µm (**A-C**), 10 mm (**D**). Abbreviation: SLAM = suspended-layer additive manufacture. Please click here to view a larger version of this figure.

Skin analogues

SLAM was also used to create a skin-like structure (**Figure 2A**) using a bioink formed from a blend of collagen I and pectin. To achieve a gradient of mechanical properties similar to those found in the skin, different proportions of pectin and collagen were used in the dermal (5% w/w pectin mixed at 2:1 with a 5 mg·mL^{-1} collagen stock) and hypodermal (5% w/w pectin mixed at 1:1 with a 5 mg·mL^{-1} collagen stock) layers. The resulting structure (**Figure 2Bi-Bii**) was well integrated following immersion in DMEM, with no sign of delamination. Importantly, there was a high level of cell viability throughout the structure (**Figure 2Biii**) following a period of 14 days of culture. Interestingly, over the period of culture, the materials stiffened[24], indicating a remodeling of the material.

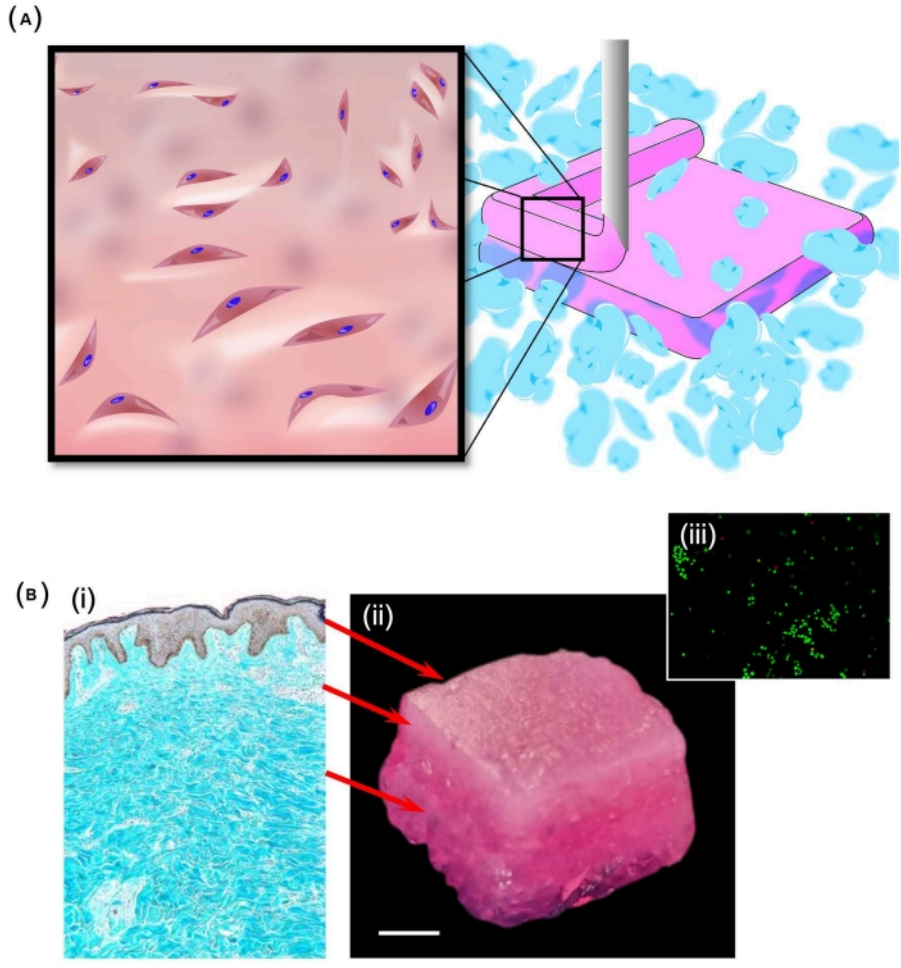

Figure 2: Production of a skin-like structure. (**A**) A schematic showing how the SLAM process was used to produce a layered structure embedded with human dermal fibroblasts. The suspending bed here was manufactured from particles formed from agarose, while the hypodermal and dermal layers were formed of varying proportions of pectin and collagen I. (**B**) The layered structure was intended to represent the trilayered structure of skin (**i**). With success in replicating this structure (**ii**), high levels of cell viability were noted throughout the samples, as shown by calcein-AM staining (**iii**). Scale bar

= 5 mm (**Bii**). Abbreviation: SLAM = suspended-layer additive manufacture. Please click here to view a larger version of this figure.

Carotid artery

To push the boundaries of the method, a selection of more complex prints was produced. In one such example, a bifurcated carotid artery was printed using 1% gellan bioink (**Figure 3A**), which was then crosslinked by extrusion of 200 mM $CaCl_2$ within the fluid gel bed (**Figure 3B**) and simply lifted from the support following gelation (**Figure 3C**). Despite precursor printing solutions exhibiting low viscosity, the supporting bed was successful in enabling production of the complex geometry. The artery retained its structure during deposition, crosslinking, and extraction (**Figure 3**), without the need to modify print codes to incorporate additional scaffolding.

Figure 3: Fabrication process of gellan carotid artery using SLAM. (**A**) Extrusion of gellan within the fluid gel bed during printing, (**B**) completed carotid artery print within the fluid gel during crosslinking, and (**C**) final carotid artery model following retrieval from fluid gel support. Scale bars = 10 mm. Please click here to view a larger version of this figure.

Discussion

Consideration of the selection of materials used for the supporting bed

During the development stage, there were various characteristics required of the supporting bed. These characteristics included: i) maintaining sufficient structure to suspend the extruded material; ii) shear thinning capacity to allow the printhead to move freely through the supporting material; iii) rapid restructuring (self-healing properties), forming support around the deposited bioink; iv) thermally stable at both room temperature and physiological temperatures; v) neutral (i.e., uncharged) material that is relatively bioinert, across a range of pH and electrolytes (ionic species and concentrations), preventing interactions with cells and charged bioinks; vi) non-toxic; and, vii) preferably from a non-animal source.

Although there are many biopolymer materials that maintain several of these inherent characteristics, with a capacity to perform suspended 3D additive manufacture without conforming to all of these characteristics[11,26,27], the intention here was to produce a supporting bed that would overcome certain practical issues associated with other supporting materials. Due to the chemical properties of agarose and, in particular, when formulated as a particulate fluid gel, all of these characteristics could be obtained.

This enabled a supporting bed that could be used across a wide variety of bioinks[23,24,25,28]. Indeed, the bioinert nature of the material provided the potential to maintain the printed structure *in situ* throughout culture, allowing sufficient timescales for many different bioinks to fully develop, without changes to the biology. Furthermore, the particulate, thinning nature allowed ease of removal from the final printed construct, while the non-toxic, non-animal origin allows the potential for rapid translation toward the clinic, overcoming barriers relating to ethical and regulatory requirements.

Considerations in the selection of materials for the bioinks

In direct-extrusion bioprinting, bioinks are deposited onto a 2D print bed. It is beneficial that monomer bioink solutions have shear-thinning behavior; however, to produce high-fidelity constructs with physiologically relevant dimensions, they must have low thixotropy and recover to sufficiently high viscosities so that they form solid filaments upon deposition[29,30,31]. With increased viscosity, the pressure required for extrusion is much higher, often negatively influencing the encapsulated cell viability[31,32]. Suspension bioprinting removes this limitation, as the extruded material is supported by the suspension bath throughout crosslinking. This development hugely increases the range of bioink formulations that can be used. For example, recent work has shown the use of low-concentration collagen solutions being printed into highly complex geometries analogous to the internal structure of the heart[33,34,35]. In the applications mentioned in this method, embedded printing allowed biomaterial inks to be chosen to best replicate the physiological environment for which they were intended, instead of for their ability to be printed.

Limitations in structure size

Throughout the biofabrication literature, it has been demonstrated that different kinds of bioprinters, driven by alternative printhead technologies, may be incorporated into embedded manufacturing techniques. The technology demonstrated here is no different, with examples that include a pneumatic micro-extrusion-based bioprinter (INKREDIBLE), as demonstrated by Senior et al., and extrusion-based bioprinters with controllable microvalves (3D Discovery)[23]. Although this makes the technology accessible to a range of users who may already own a bioprinter, limitations on the attainable size of the structure are ultimately dependent on the bioprinter specifications in question. Initially, the main restriction upon the generation of large structures is defined by the size of the print bed, the limits of X, Y, and Z trajectories, and also the size of the vessel in which the supporting fluid gel is contained.

Limitations in resolution

When fabricating intricate, micrometer-sized structures, the resulting resolution is highly dependent on the precision of the printer (control over step size, degree of extrusion), the internal diameter of the print nozzle, and a range of adjustable software parameters, including print speed, print pressure, and flow velocity[36]. In addition, control over the droplet size appears to be critical to facilitating the generation of high-resolution structures, with the best results observed in extrusion printers with a controllable microvalve. Ultimately, when all parameters are optimized, print resolutions can be achieved to match, or even be less than, the inner diameter of extrusion nozzles, with the deposited filament on the order of the micrometer scale[37]. This is, however, reliant on the optimization of all the printing parameters previously mentioned, and resolution can be considerably limited by the printing mechanism and precision. Pneumatic extrusion, for example, does not appear to allow for the same

printing resolution as extrusion with a controllable microvalve. There is, therefore, a potential cost implication to achieve the maximum printing resolution, as such systems incur a significantly increased expense to the user.

Future outlook and potential

At the moment, there is much interest around the use of suspended manufacturing processes to allow for the production of complex soft structures containing embedded cells, and there will undoubtedly be significant advances in the coming years. Continuous advancement in improving print resolution is given, although it remains to be seen how necessary this will be, given that the majority of biological systems are able to rearrange themselves on a molecular level. While the focus of interest in the media is around the use of 3D printed tissues to directly replace human tissues following injury or disease, any robust medical procedures enabled by these processes are some years away[38,39]. It is more likely that the impact of these complex culture systems will be in the screening of drugs or even used as tools, to enhance our understanding of biological processes[38]. In particular, developmental biology could greatly benefit here, where precise control over the special deposition of molecules will allow researchers to explore the role of multifactorial systems on tissue development processes.

Disclosures

The authors have no conflicts of interest to declare.

Acknowledgments

The authors would like to thank the EPSRC (EP/L016346/1), MRC, and the Doctoral Training Alliance Biosciences for Health for funding and supporting this work.

References

1. Lee, K. Y., Mooney, D. J. Hydrogels for tissue engineering. *Chemical Reviews.* **101** (7), 1869-1880 (2001).
2. Caliari, S. R., Burdick, J. A. A practical guide to hydrogels for cell culture. *Nature Methods.* **13** (5), 405-414 (2016).
3. Tibbitt, M. W., Anseth, K. S. Hydrogels as extracellular matrix mimics for 3D cell culture. *Biotechnology and Bioengineering.* **103** (4), 655-663 (2009).
4. Drury, J. L., Mooney, D. J. Hydrogels for tissue engineering: scaffold design variables and applications. *Biomaterials.* **24** (24), 4337-4351 (2003).
5. Iordachescu, A. et al. An in vitro model for the development of mature bone containing an osteocyte network. *Advanced Biosystems.* **2** (2), 1700156 (2018).
6. Zhang, C. et al. Hydrogel cryopreservation system: an effective method for cell storage. *International Journal of Molecular Sciences.* **19** (11), 3330 (2018).
7. McCormack, A., Highley, C. B., Leslie, N. R., Melchels, F. P. W. 3D printing in suspension baths: keeping the promises of bioprinting afloat. *Trends in Biotechnology.* **38** (6), 584-593 (2020).
8. Cheng, W., Zhang, J., Liu, J., Yu, Z. Granular hydrogels for 3D bioprinting applications. *View.* **1** (3), 20200060 (2020).
9. Lieben, L. The future of 3D printing of human tissues is taking shape. *Nature Reviews Rheumatology.* **12** (4), 191-191 (2016).
10. Bhattacharjee, T. et al. Writing in the granular gel medium. *Science Advances.* **1** (8), e1500655 (2015).
11. Hinton, T. J. et al. Three-dimensional printing of complex biological structures by freeform reversible embedding

of suspended hydrogels. *Science Advances.* **1** (9), e1500758 (2015).

12. Zarrintaj, P. et al. Agarose-based biomaterials for tissue engineering. *Carbohydrate Polymers.* **187**, 66-84 (2018).
13. te Nijenhuis, K. *Thermoreversible Networks: Viscoelastic Properties and Structure of Gels.* Springer, Berlin. 194-202 (1997).
14. Norton, I. T., Jarvis, D. A., Foster, T. J. A molecular model for the formation and properties of fluid gels. *International Journal of Biological Macromolecules.* **26** (4), 255-261 (1999).
15. Fernández Farrés, I., Moakes, R. J. A., Norton, I. T. Designing biopolymer fluid gels: A microstructural approach. *Food Hydrocolloids.* **42**, 362-372 (2014).
16. Cooke, M. E. et al. Structuring of hydrogels across multiple length scales for biomedical applications. *Advanced Materials.* **30** (14), 1705013 (2018).
17. Foster, N. C., Allen, P., El Haj, A. J., Grover, L. M., Moakes, R. J. A. Tailoring therapeutic responses via engineering microenvironments with a novel synthetic fluid gel. *Advanced Healthcare Materials.* **10** (16), 2100622 (2021).
18. Ellis, A. L., Norton, A. B., Mills, T. B., Norton, I. T. Stabilisation of foams by agar gel particles. *Food Hydrocolloids.* **73**, 222-228 (2017).
19. Ghebremedhin, M., Seiffert, S., Vilgis, T. A. Physics of agarose fluid gels: Rheological properties and microstructure. *Current Research in Food Science.* **4**, 436-448 (2021).
20. Garrec, D. A., Norton, I. T. Understanding fluid gel formation and properties. *Journal of Food Engineering.* **112** (3), 175-182 (2012).
21. Garrec, D. A., Guthrie, B., Norton, I. T. Kappa carrageenan fluid gel material properties. Part 1: Rheology. *Food Hydrocolloids.* **33** (1), 151-159 (2013).
22. Adams, S., Frith, W. J., Stokes, J. R. Influence of particle modulus on the rheological properties of agar microgel suspensions. *Journal of Rheology.* **48** (6), 1195-1213 (2004).
23. Senior, J. J., Cooke, M. E., Grover, L. M., Smith, A. M. Fabrication of complex hydrogel structures using suspended layer additive manufacturing (SLAM). *Advanced Functional Materials.* **29** (49), 1904845 (2019).
24. Moakes, R. J. A. et al. A suspended layer additive manufacturing approach to the bioprinting of tri-layered skin equivalents. *APL Bioengineering.* **5** (4), 046103 (2021).
25. Moxon, S. R. et al. Suspended manufacture of biological structures. *Advanced Materials.* **29** (13), 1605594 (2017).
26. Noor, N. et al. 3D Printing of personalized thick and perfusable cardiac patches and hearts. *Advanced Science.* **6** (11), 1900344 (2019).
27. Compaan, A. M., Song, K., Huang, Y. Gellan fluid gel as a versatile support bath material for fluid extrusion bioprinting. *ACS Applied Materials & Interfaces.* **11** (6), 5714-5726 (2019).
28. Moxon, S. R. et al. Blended alginate/collagen hydrogels promote neurogenesis and neuronal maturation. *Materials Science and Engineering: C.* **104**, 109904 (2019).
29. Hölzl, K. et al. Bioink properties before, during and after 3D bioprinting. *Biofabrication.* **8** (3), 032002 (2016).

30. Chimene, D., Lennox, K. K., Kaunas, R. R., Gaharwar, A. K. Advanced bioinks for 3D printing: a materials science perspective. *Annals of Biomedical Engineering.* **44** (6), 2090-2102 (2016).

31. Schwab, A. et al. Printability and shape fidelity of bioinks in 3D bioprinting. *Chemical Reviews.* **120** (19), 11028-11055 (2020).

32. Rutz, A. L., Lewis, P. L., Shah, R. N. Toward next-generation bioinks: Tuning material properties pre- and post-printing to optimize cell viability. *MRS Bulletin.* **42** (8), 563-570 (2017).

33. Mosadegh, B., Xiong, G., Dunham, S., Min, J. K. Current progress in 3D printing for cardiovascular tissue engineering. *Biomedical Materials.* **10** (3), 034002 (2015).

34. Zhou, K., Sun, Y., Yang, J., Mao, H., Gu, Z. Hydrogels for 3D embedded bioprinting: a focused review on bioinks and support baths. *Journal of Materials Chemistry B.* **10** (12), 1897-1907 (2022).

35. Lee, A. et al. 3D bioprinting of collagen to rebuild components of the human heart. *Science.* **365** (6452), 482-487 (2019).

36. Kyle, S., Jessop, Z. M., Al-Sabah, A., Whitaker, I. S. 'Printability' of candidate biomaterials for extrusion based 3D printing: state-of-the-art. *Advanced Healthcare Materials.* **6** (16), 1700264 (2017).

37. Hinton, T. J., Lee, A., Feinberg, A. W. 3D bioprinting from the micrometer to millimeter length scales: Size does matter. *Current Opinion in Biomedical Engineering.* **1**, 31-37 (2017).

38. Seoane-Viaño, I., Trenfield, S. J., Basit, A. W., Goyanes, A. Translating 3D printed pharmaceuticals: From hype to real-world clinical applications. *Advanced Drug Delivery Reviews.* **174**, 553-575 (2021).

39. Jovic, T. H., Combellack, E. J., Jessop, Z. M., Whitaker, I. S. 3D bioprinting and the future of surgery. *Frontiers in Surgery.* **7**, 609836 (2020).